THE ASTROPHYSICAL JOURNAL, 447:742–751, 1995 July 10

THERMAL STRUCTURE OF MIXING LAYERS IN BIPOLAR OUTFLOWS

SUSANA LIZANO[1] AND CARLO GIOVANARDI[2]
Received 1994 September 21; accepted 1995 January 12

ABSTRACT

Assuming that molecular outflows from young low-mass stars are driven by fast neutral atomic winds, we further explore the possibility that these winds interact with the ambient cloud through entrainment of molecular material. This paper is aimed to determine the energy balance and the resulting thermal structure of the entrainment region.

We model the entrainment region as a mixing layer along the walls of a cavity within the cloud itself. We make use of the 21 cm H I spectral profiles observed in L1551 to specify a priori the overall geometry of the flow and the amount of entrainment at each point. Assuming momentum conservation in the layer, we determine—in a single parcel approximation—the radial temperature profile of the mixing layer.

We find that, with a reasonable choice of assumptions, the temperature in these regions is between 3000 and 5000 K. This results from heating due to the dissipation of wind kinetic energy as it decelerates outward due to mass entrainment, and from cooling by rovibrational emission of molecular hydrogen. We find that, because of the low density, short crossing time, and replenishment from the cloud, the H_2 is not dissociated and acts as the main coolant in the layer. Even taking into account nonthermal impacts, due to the low density, the thermal coupling between gas and dust is low and results in much lower dust temperatures (10–20 K) through most of the mixing layer. For the same reason dust is not an effective coolant. In the case of L1551 the H_2 emission from the mixing layer, e.g., in the $v = 1$–0 $S(1)$ line, should be spread over most of the CO lobes and within the detection limits of current (arcminute resolution) near-infrared spectrographs.

Subject headings: circumstellar matter — ISM: jets and outflows — radio lines: ISM — stars: mass loss — stars: pre–main-sequence

1. INTRODUCTION

Mass ejection appears to be a common phenomenon during the protostellar and pre–main-sequence (PMS) evolutionary phases, to the point that it is believed to be crucial to the star formation process (Shu, Adams, & Lizano 1987). In optically visible PMS stars, such as T Tauri stars, mass outflow was first inferred from the P Cygni profiles of strong emission lines (Herbig 1962). The velocity of these stellar winds can exceed 200 km s^{-1}, which is comparable to the escape velocity from the star. At the same time, CO mapping at millimeter wavelengths of both visible PMS objects and deeply embedded far-infrared sources has revealed molecular outflows extending on parsec scales with velocities of some tens of km s^{-1} (Lada 1985; Bally & Lane 1991). It was first proposed by Snell, Loren, & Plambeck (1980) to unify the two phenomena in a scenario where the molecular outflow is ambient molecular material driven by the fast stellar wind. This view has gained considerable support in the last years due to the following observations.

In the case of low-mass PMS objects, the stellar winds were expected to be mostly atomic and neutral (Natta et al. 1987; Rawlings, Williams, & Cantó 1988; Ruden, Glassgold, & Shu 1990). These winds have been detected directly in the 21 cm H I line in the low-mass young stellar objects (YSOs) HH 7–11, L1551, and T Tau (Lizano et al. 1989; Giovanardi et al. 1992, hereafter Paper I; Rodríguez et al. 1990; Ruiz, Alonso, & Mirabel 1992) and also from the high-mass stars exciting NGC 2071 and DR 21 (Bally & Stark 1983; Russell et al. 1992). In the case of L1551, the best studied case, the atomic stellar wind is found to be coextensive with the (red) CO lobe and slowly decelerating away from IRS 5. High sensitivity CO studies have detected faint components with velocities up to 150 km s^{-1} in several outflows, e.g., in HH 7–11 (Lizano et al. 1988; Bachiller & Cernicharo 1990). This is the so-called extremely high velocity CO which streams out at roughly the same velocity as the stellar wind (see also Koo 1989). In addition, other phenomena in star-forming regions are usually interpreted as being the result of the interaction between fast moving flows and the ambient cloud: Herbig-Haro objects, optical jets, high-velocity water masers, and extended IR emission from warm dust.

From the above cited studies of neutral winds one can deduce that low-mass sources have mass-loss rates $\dot{M} \sim 10^{-5}$ to 10^{-6} $M_\odot$ yr^{-1} and velocities $v_w \sim 200$ km s^{-1}. Instead, massive sources have $\dot{M} \sim 10^{-3}$ $M_\odot$ yr^{-1} and detected[3] wind velocities $v_w \sim 90$–120 km s^{-1}. Such fast massive winds can entrain and accelerate material from the surrounding molecular cloud in a mixing layer such as those studied in the context of optical jets, by Cantó & Raga (1991, hereafter CR91). In Paper I we were able to reproduce the H I profiles observed at different positions in L1551 by modeling the flow as a free-flowing conical wind plus a decelerating layer along the walls of the cone. One of the most direct explanations for such a deceleration is to advocate mass entrainment through the walls with the conservation of linear momentum of the stellar wind (or, more precisely, the flux of momentum per unit solid angle). Our model was parameterized to reproduce the spectral pro-

[1] Instituto de Astronomía, UNAM, Apdo. Postal 70-264, 04510 México, D.F., México.
[2] Osservatorio Astrofisico di Arcetri and CAISMI-CNR, Largo E. Fermi 5, I-50125 Firenze, Italy.

[3] Since these sources have been observed at the VLA, while the low-mass sources were observed at Arecibo with higher sensitivity, it is possible that existing higher wind velocities have not been detected; see Rodríguez et al. 1990.

files and no attempt was made to model the actual physical structure of the resulting layer. In particular, if one considers that the total kinetic luminosity of the L1551 wind is about 17 $L_\odot$ (Paper I), in order to decelerate it appreciably, an energy of the order of a few $L_\odot$ has to be dissipated. In the absence of efficient cooling mechanisms this source of heating could heat the gas and ionize it easily, a situation which is not supported by the observations, especially by the presence of a high velocity and an extremely high velocity molecular phase.

In the present paper, we intend to study the thermal structure these mixing layers should have, given the wind properties of the neutral winds from low-mass stars, in particular those observed in L1551. In our model of the mixing layer we assume an ad hoc parameterization for the amount of mass entrainment needed at each point within the wind and then determine the radial temperature profile by taking into account the various cooling agents appropriate to such media.

2. MODEL

We consider the steady state mixing layer model used in Paper I. The overall geometry of the flow is illustrated in Figure 1. The flow, assumed to be azimuthally symmetric, is confined within a cone with vertex at O, the origin of the wind, and opening half-angle α. Outside the cone ($\theta > \alpha$) is the ambient molecular cloud, supposed to be spherically symmetric, at rest, isothermal, and with mass density profile $\rho_c \propto r^{-\gamma}$, where r is the distance from O and γ a constant exponent. Between α and θ_{ent} is the mixing layer, that is, the region where cloud molecular material, entrained from the "wall" ($\theta = \alpha$), mixes with (atomic) wind material; θ_{ent} is the inner limit to the entrainment and to any perturbation on the wind by the ambient medium. The paraxial region ($\theta < \theta_{ent}$) is occupied by the unperturbed, radially streaming wind.[4]

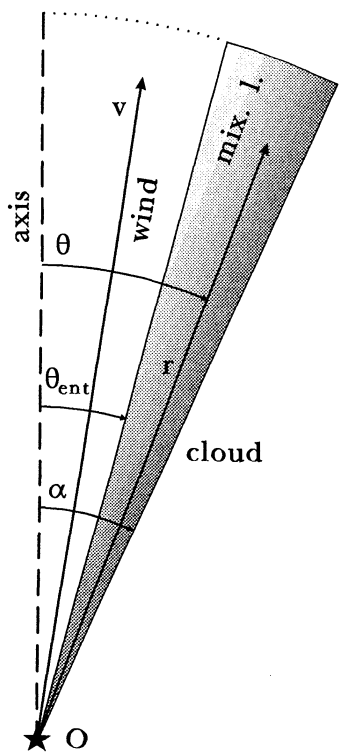

FIG. 1.—Overall geometry of the flow. We consider a cone of semiaperture α centered on the star in the origin O. The mixing layer is the shaded region between θ_{ent} and α. Out of the cone is the ambient molecular cloud, while the wind flows freely in the inner ($\theta < \theta_{ent}$) region. In the wind region, the flow is radial. In the mixing layer there is also a transversal mass transfer with velocity $v_\theta \ll v$. The cloud is at rest and has a radial density gradient $\rho \propto r^{-\gamma}$.

The radial velocity is $v(r, \theta)$. Note that within the mixing layer the flow is not completely radial; due to the entrainment there is a transfer of mass toward the axis with velocity $v_\theta(r, \theta)$. Since the radial flow is highly supersonic, while the transversal transfer is due in this scheme to a diffusion process, we will always assume $v_\theta \ll v$. Following Paper I, if v_0 is the wind injection velocity at O (independent of θ), momentum conservation in the radial direction implies that the velocity at each point in the flow is given by

$$v(r, \theta) = \frac{v_0}{1 + \epsilon(r, \theta)}, \tag{1}$$

where we have introduced an entrainment function $\epsilon(r, \theta) \geq 0$. In the case of an isothermal cloud with a power-law density profile, $\rho_c \propto r^{-\gamma}$,

$$\epsilon(r, \theta) = \left(\frac{r}{r_{ent}}\right)^{2-\gamma} F(\theta), \tag{2}$$

where r_{ent}, the entrainment radius, is a scale length defining the efficiency of the entrainment process. Because of the decrease in the molecular cloud density, less mass is entrained as the flow moves away from the source. We have assumed that $\epsilon(r, \theta)$ is factorable[5] and that $F(\theta)$ describes the run with θ, with the constraint $F(\theta_{ent}) = 0$. $F(\theta)$ depends on the detailed mass transfer in the θ direction. For simplicity in Paper I we adopted a linear relation for $F(\theta)$. Then

$$\epsilon(r, \theta) = \left(\frac{r}{r_{ent}}\right)^{2-\gamma} \left(\frac{\theta - \theta_{ent}}{\alpha - \theta_{ent}}\right), \tag{3}$$

which is equivalent to the quasi-laminar "Couette flow" assumed by CR91 for their parallel flows.

If $\dot{A}_1$ is the initial mass-loss rate per unit solid angle, that is, the loss rate in the driving atomic wind which we assume independent of θ, the density at each point of the flow is given by

$$\rho(r, \theta) = \frac{\dot{A}_1 v_0}{r^2 v^2(r, \theta)} = \frac{\dot{A}_2}{r^2 v^2(r, \theta)}, \tag{4}$$

where $\dot{A}_2$ is the (constant) momentum flux per steradian.

This model is a parameterization of the process of mass entrainment in an isothermal, inhomogeneous molecular cloud as opposed to self-consistent models of mixing layers, such as those of CR91. We simplify the model even further by taking a mean velocity and density in the θ direction with $F(\theta) = 0.5$ in equation (2), and then treat the energy equation in a single parcel approximation as a function of radial distance only. At a fixed geometry, a given model is characterized by the initial wind velocity v_0, the wind mass loss rate $\dot{A}_1$, the radius r_{ent} of

[4] In reality, the borders of the various regions are not expected to have constant opening angles. The layer-cloud interface will open out with radius into the cloud while the wind-layer interface will close into the wind (CR91). Such deviations depend on the physical parameters of the wind + cloud system, namely densities, temperatures, and Mach number. From calculations and simulations we are presently performing it appears that, in the range of parameters of interest, most of the angular variations are confined to the very initial region of the flow; this is due to the high Mach number (> 100) and to the gradient in the cloud density.

[5] This is strictly true only in the case of instant transversal mixing.

entrainment, and by the cloud density exponent γ. In particular, for the results presented in § 4, we chose the parameters that best fitted the H I profiles of L1551 in Paper I.

Assuming that all the gas components (atoms, electrons, and molecules) but the dust, have the same temperature, we write the energy equation in the form

$$\rho(\boldsymbol{v}\cdot\nabla)(c_v T) = \Gamma - \Lambda - P\nabla\cdot\boldsymbol{v}\,, \tag{5}$$

where T and P are the gas temperature and pressure, c_v is the translational specific heat at constant volume per unit mass, Γ includes all the heating mechanisms (ergs cm^{-3} s^{-1}) and Λ all the cooling mechanisms. The last term on the right-hand side represents the mechanical work performed by pressure stresses (we will ignore any viscosity and shear), the term is usually referred to as adiabatic expansion. The gas is assumed to be a perfect gas with a variable molecular weight according to its local composition.

3. HEATING AND COOLING

In this section, we briefly outline the various mechanisms included to evaluate the Γ and Λ terms in equation (5).

3.1. *Heating*

Due to the entrainment of mass while conserving momentum, the stellar wind is radially decelerated within the mixing layer. As a result, the kinetic energy flux (per unit solid angle) decreases with radius and part of the wind kinetic luminosity must be converted to heat and dissipated. Probably a substantial fraction will first excite supersonic turbulent motions in the layer which will be subsequently damped and converted into thermal energy. It is argued by CR91 that due to this mechanism the most probable situation is one of sonic turbulence throughout the layer. It is difficult to assess the details of such energy cascade, and we will simply parameterize the amount actually converted into thermal motions by introducing a heating factor η as the ratio between the contribution to the thermal energy with respect to the total thermal + turbulent energy deposition, so that η is the fraction of dissipated energy actually available to heat the gas ($0 \geq \eta \geq 1$). We will also assume a constant η through the mixing layer. The entrainment heating function is then given by

$$\Gamma_{\rm ent} = -\eta\nabla\cdot(\rho\boldsymbol{v}\tfrac{1}{2}v^2)\,, \tag{6}$$

where the right-hand side is just the divergence of the kinetic energy flux and is positive if the wind decelerates outward. We have neglected the viscous heating due to the shear in the mixing layer since it is smaller than $\Gamma_{\rm ent}$ by a factor $\sim c/v$, where c—the sound speed in the layer itself—turns out to be, in our models, of the order of ~ 6 km s^{-1}.

We will ignore other sources of heating such as cosmic rays or the radiation field from the central star. In fact, even considering the most favorable values for the cosmic-ray flux and energy distribution, it is difficult to achieve heating rates, via ionization of neutral H and He, in excess of $5\times10^{-27}n_{\rm H}$ (ergs s^{-1} cm^{-3}), where $n_{\rm H}$ is the neutral H number density (Dalgarno & McCray 1972; Spitzer 1978); the heating rate is somewhat higher but similar for ionization of H_2 molecules. Within our range of parameters, heating by cosmic rays will always be negligible compared to the effect of mass entrainment. As for the stellar radiation, due to the low effective temperature (4000–5000 K) of low-mass YSOs, the radiation field will have a predominantly nonionizing character. Therefore, its contribution for the direct heating of the gas will be ignored but it will be included when computing the dust temperature and then taken into account via the gas-dust interaction. Finally, we have ignored the contribution of exothermic molecular reactions and molecule formation, their importance as heating agents being confined to the high-density circumstellar region within a few stellar radii (e.g., Ruden et al. 1990).

3.2. *Cooling*

As cooling sources we have considered (1) vibrational/rotational emission by H_2, (2) collisional dissociation of H_2, (3) rotational/vibrational emission by molecules with dipole moments, (4) atomic line emission, and (5) dust continuum emission.

3.2.1. *Emission and Dissociation*

We have assumed that the content of molecular hydrogen in the layer is determined by a balance between injection of fresh H_2 from the cloud (i.e., the entrained material) and collisional dissociation in the high-temperature environment of the layer itself. In addition, as already noted, we assume the same temperature for the various phases (except for dust) and a single parcel description. For this to be justified the dissociation time $\tau_{\rm diss}(r)$ must exceed both the thermalization time $\tau_{\rm rh}(r)$ and the time for transversal mixing $\tau_\theta(r)$ within the layer, conditions which are largely satisfied through most of the models considered, as it will be shown in § 4.

We can then write a continuity equation for the molecular mass density $\rho_{\rm H_2}$ in the form

$$\nabla\cdot[\rho_{\rm H_2}(r)\boldsymbol{v}(r)] = I(r) - D(r)\,, \tag{7}$$

where $\rho_{\rm H_2}$ is the molecular mass density, $I(r)$ is the H_2 mass injection rate, and $D(r)$ the destruction rate by collisional dissociation. Assuming that all the entrained material is molecular, we have $I = \nabla\cdot\rho\boldsymbol{v}$, and so the injection term can be easily derived from equations (1) and (4). The mass dissociation rate is $D = 2m_{\rm H}R_d$, where $m_{\rm H}$ is the hydrogen mass and R_d the dissociation rate (cm^{-3} s^{-1}). To compute R_d we have used the analytic fits by Lepp & Shull (1983) with the revision of Mac Low & Shull (1986), and the rates of Dove & Mandy (1986) for low densities; R_d is a function of the temperature T, of the H I number density $n_{\rm H}$, and of the H_2 number density $n_{\rm H_2}$.[6]

The total H_2 line cooling was computed following the prescription of Lepp & Shull (1983), and the dissociation cooling by attributing to each dissociation event the ground state energy, that is, $\Lambda_{\rm diss} = (4.477\ {\rm eV})R_d$.

3.2.2. *Molecules with Dipole Moments*

Given the large velocity gradients in the region of the flow and particularly within the mixing layer, the molecular cooling functions were computed in an optically thin approximation.

To evaluate the contribution to Λ by heteropolar molecules we have followed the treatment by Hollenbach & McKee (1979) for rotational transitions. The species included are ^{12}CO, ^{13}CO, HD, H_2O, OH, and HCl. We included the correction for ^{12}CO and ^{13}CO cooling by McKee et al. (1982). For low densities, the H_2O cooling rate coefficient agrees well with that of Neufeld & Kaufman (1989).

We included vibrational cooling via the excitation of the $v = 1$ state of OH as

$$\Lambda_{v,\rm OH} = n_{\rm OH}(n_{\rm H}\gamma_{01}^{\rm H} + n_{\rm H_2}\gamma_{01}^{\rm H_2})\Delta E_{01}\,, \tag{8}$$

[6] Due to the low ionization fraction in these layers, we ignore the dissociation by electron impact.

with the estimated rate coefficients in $cm^3\ s^{-1}$ (A. Dalgarno, private communication) given by

$$\gamma_{01}^{H} = 1 \times 10^{-14} T \exp\left(-\frac{\Delta E_{01}}{kT}\right)$$

and

$$\gamma_{01}^{H_2} = 1 \times 10^{-15} T \exp\left(-\frac{\Delta E_{01}}{kT}\right), \quad (9)$$

where $\Delta E_{01}/k = 5136$ K and n_{OH} is the number density of OH. We also included the vibrational cooling of H_2O as given by Hollenbach & McKee (1989).

Abundances and molecular parameters were taken from the list compiled by Hollenbach & McKee (1979). We have also assumed that molecules are provided only by the entrained material and that they are not formed or dissociated locally in the layer. We note that all the approximations introduced in the evaluation of the molecular emission (except H_2), tend to overestimate such cooling.

3.2.3. *Atomic Cooling*

We include in this single term all the line and continuum emission by atoms and ions which are relevant to interstellar cooling. To evaluate this term we used a numerical interpolation of the curves of Dalgarno & McCray (1972), which depend on temperature, atomic density, and electron density (or ionization fraction). We have assumed that both atoms and ions are contained only in the atomic fraction of the gas; the atomic content at a certain radius is contributed by the original wind plus the dissociated entrained material. The only processes considered to estimate the electron density were hydrogen collisional ionization from the ground level and radiative recombination; metallic electrons were only taken into account to fix a lower limit (10^{-6}) to the value of the ionization fraction $x_e = n_e/n_H$, where n_e is the electron number density and n_H the density of neutral plus ionized hydrogen. We can then write a continuity equation for the electrons in the form:

$$\nabla \cdot [n_e(r)\mathbf{v}(r)] = \mathscr{C}_{eH}(r) - R_{eH}(r)\,; \quad (10)$$

here $\mathscr{C}_{eH}$ is the rate of H collisional ionization by electron impact and R_{eH} is the rate of recombination (per cm^3) to all levels but $n = 1$. Equation (10) has been integrated under the hypothesis that all the neutral hydrogen is in the ground state.

3.2.4. *Cooling by Dust*

In our models the dust turned out to be substantially cooler than the gas in most of the flow region. It is therefore included here among the sources of cooling.

To include the effect of nonthermal velocities, we adopted a formulation similar to that of Draine (1980) which is detailed in the Appendix. The dust temperature T_{gr} in the mixing layer is computed including collisions with gas particles and allowing for diffuse background radiation as well as diluted stellar radiation. In addition to the usual dust parameters (such as abundance, size, absorption efficiency, etc.), we then need to specify both background and star temperatures. In our formulation the gas to dust thermal coupling is adjusted by means of two accommodation factors.

We assume (1) that the original stellar wind contains no dust, that is, the dust in the layer is contributed only by entrained material; (2) that no dust grains condense in the flow; (3) that grains are not sputtered and destroyed. Regarding the relative motion of gas and dust, we consider the two limiting cases of no relative motion and of purely mechanical drag. The first case is likely to occur if grains are charged and then linked to the gas by the (turbulent) magnetic field in the layer. The second one is pertinent to neutral grains[7] injected at zero velocity and dragged by the gas in the mixing layer. For the conditions considered in our model, the second case is probably more appropriate: the grains are slowly accelerated and the impact velocity between gas and dust particles deviates considerably from the thermal speed.

Considering the above heating and cooling sources and the simple flow model presented in § 2, the radial temperature profile $T(r)$ of the mixing layer was determined by integrating the system comprised of (1) the thermal energy equation, equation (5); (2) the continuity equation for the molecular mass density, equation (7); (3) a continuity equation for the dust content as described in the Appendix; (4) the continuity equation for the electron density, equation (10); and (5) the dust temperature equation (see Appendix). The results are presented in the following section.

4. RESULTS

The following calculations were performed for a wind mass-loss rate $\dot{A} = 6 \times 10^{-6}\ M_\odot\ yr^{-1}\ sr^{-1}$, a wind velocity $v_0 = 200$ km s^{-1}, an entrainment radius $r_{ent} = 0.08$ pc. As for the angles, we fixed the wind opening angle $\alpha = 20°$ and the entrainment angle $\theta_{ent} = 12°$. We considered a molecular cloud with a power-law density profile $\rho_c \propto r^{-1.5}$. Although with sizable uncertainties ($\sim 20\%$), these are the values which produced the best fit to the H I spectral profiles observed in the source L1551 (Paper I), which are the only direct evidence so far of a spatially resolved neutral wind in a OMS object. Since it is difficult to decide where the entrainment process begins, if such a point could be defined, we chose to start the integration at 100 AU and integrate up to 0.5 pc (the size of the CO lobes in L1551). The initial gas temperature in the mixing layer is taken to be 10 K; in fact, models of the chemistry of winds from low-mass protostars show that such winds become very cold (before the entrainment process begins) due to adiabatic expansion (e.g., Ruden et al. 1990). The results presented in what follows do not depend on this initial temperature. The gas temperature in the mixing layer does depend on which fraction of the entrainment energy goes into heating of the gas. For the heating factor η in equation (6) we considered two possible values: $\eta = 0.5$ (equipartition between thermal and turbulent energy) and $\eta = 1.0$ (negligible energy goes into turbulent motions). Finally, we set the initial ionization fraction equal to the one expected in the stellar wind of a low mass PMS star $x_e(r = 0) = 1 \times 10^{-3}$ (Natta et al. 1988). As expected, the ionization fraction freezes out to $x_e \sim 5 \times 10^{-4}$ when the density has dropped below $10^6\ cm^{-3}$; that is, at a distance $r \sim 10^{-3}$ pc.

As has been noted in § 3.2.1, we can define at each radius three characteristic times: the dissociation time τ_{diss}, defined as the ratio between the molecular density and the collisional mass dissociation rate; the thermalization time τ_{th}, defined as the average time between collisions among gas particles; and the transverse crossing time τ_θ in case of sonic turbulence, defined as the local thickness of the layer (from θ_{ent} to α) divided by the local sound speed in the layer. Figure 2 shows

[7] As could be the case, given the low electron density and low UV field, in large and dense molecular clouds.

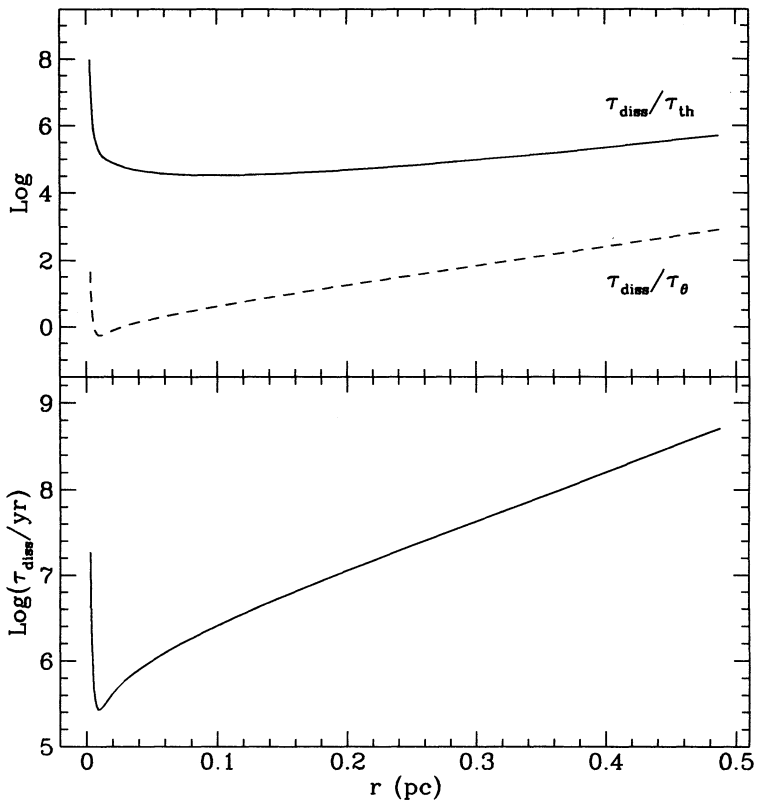

FIG. 2.—Characteristic times vs. distance r: τ_{diss} is the dissociation time defined as the ratio between the molecular density and the collisional mass dissociation rate; τ_{th} is the thermalization time, defined as the average time between collisions among gas particles; τ_{θ} is the transverse crossing time, defined as the local thickness of the layer (from θ_{ent} to α) divided by its local sound speed. τ_{diss} exceeds both τ_{th} and τ_{θ}. Moreover, as it appears from the values in the lower panel, τ_{diss} exceeds the radial crossing time of the flow which is $\sim$2000 yr.

the behavior of such characteristic times versus distance to the source r. The dissociation time largely exceeds τ_{th}, thus justifying the assumption of the same temperature for all the gas components; it also exceeds τ_{θ} over most of the flow region showing that, from this point of view, the layer can be treated in a single parcel scheme. At the same time, the value of τ_{diss} (in the lower panel) is invariably longer than the radial crossing time, and, therefore, the dissociation process and the resulting molecular content cannot be treated locally but rather necessitate the integration of a full continuity equation such as equation (7). The model in Figure 2 has a heating factor $\eta = 0.5$.

Figure 3 shows the run of the cooling functions for the different coolants described in § 3 as a function of the distance from the central star. Entrainment is the only heating source considered and is shown as the upper solid line. The various coolants are shown as dashed lines: (H2) rotational/vibrational emission of H_2; (Mol) rotational lines of molecules with dipole moments plus the first vibrational transition of OH and H_2O (this vibrational cooling was less than 1% of the rotational line cooling); (Ad) adiabatic expansion; (M) atomic cooling, includes H, He, and metals (allowed and forbidden transitions); (D) dissociation of H_2; (G) dust grains cooling. The upper panel shows the model with heating factor $\eta = 1.0$, and the lower panel shows the case for $\eta = 0.5$. This graph shows that in this model, H_2 line emission is the most important coolant in the mixing layer. This is true everywhere but for the innermost part of the flow ($r < 3 \times 10^{-3}$ pc) where radiation by atoms is dominant. Obviously this results from the hypothesis of a fully atomic wind; the rapid decay of atomic radiation is mainly due to the lowering of the electron density with r. There are several reasons for the preponderance of H_2 cooling: (1) given the conditions of low density in the mixing layer, collisional dissociation of H_2 is suppressed by radiative stabilization of the population of high vibrational levels (Lepp & Shull 1983); (2) the wind radial crossing time is short compared to the H_2 dissociation time; and (3) fresh molecular material is entrained at each radius. The entrained molecular fraction $\chi_{H_2 e}$, defined as the ratio between the local molecular density ρ_{H_2} and the contribution to the total density by the mass entrained up to that point $\chi_{H_2 e} = \rho_{H_2}/\rho_{entrained}$, is shown in the upper panel of Figure 4 as a function of distance to the central source. The entrained material remains almost completely molecular. The solid line corresponds to a heating factor $\eta = 1.0$ and the broken line to $\eta = 0.5$. The lower panel shows the molecular fraction defined as the fraction of H_2 with respect to the *total* density $\chi_{H_2} = \rho_{H_2}/\rho$. This curve shows how the molecular fraction increases with distance r due to the low dissociation and the replenishment of molecular material by entrainment.

The energy balance results in the temperature profiles shown in Figure 5. The upper panel shows the gas temperature as a function of distance to the source. Independently of the initial temperature, the mixing layer achieves temperatures of a few thousand degrees. Instead, the lower panel shows that the dust remains cold because the transfer of energy by collisions with the gas particles is very inefficient at low densities. This particular model assumes a background field temperature $T_B = 3$ K, a stellar temperature $T_* = 5000$ K, and a sticking approx-

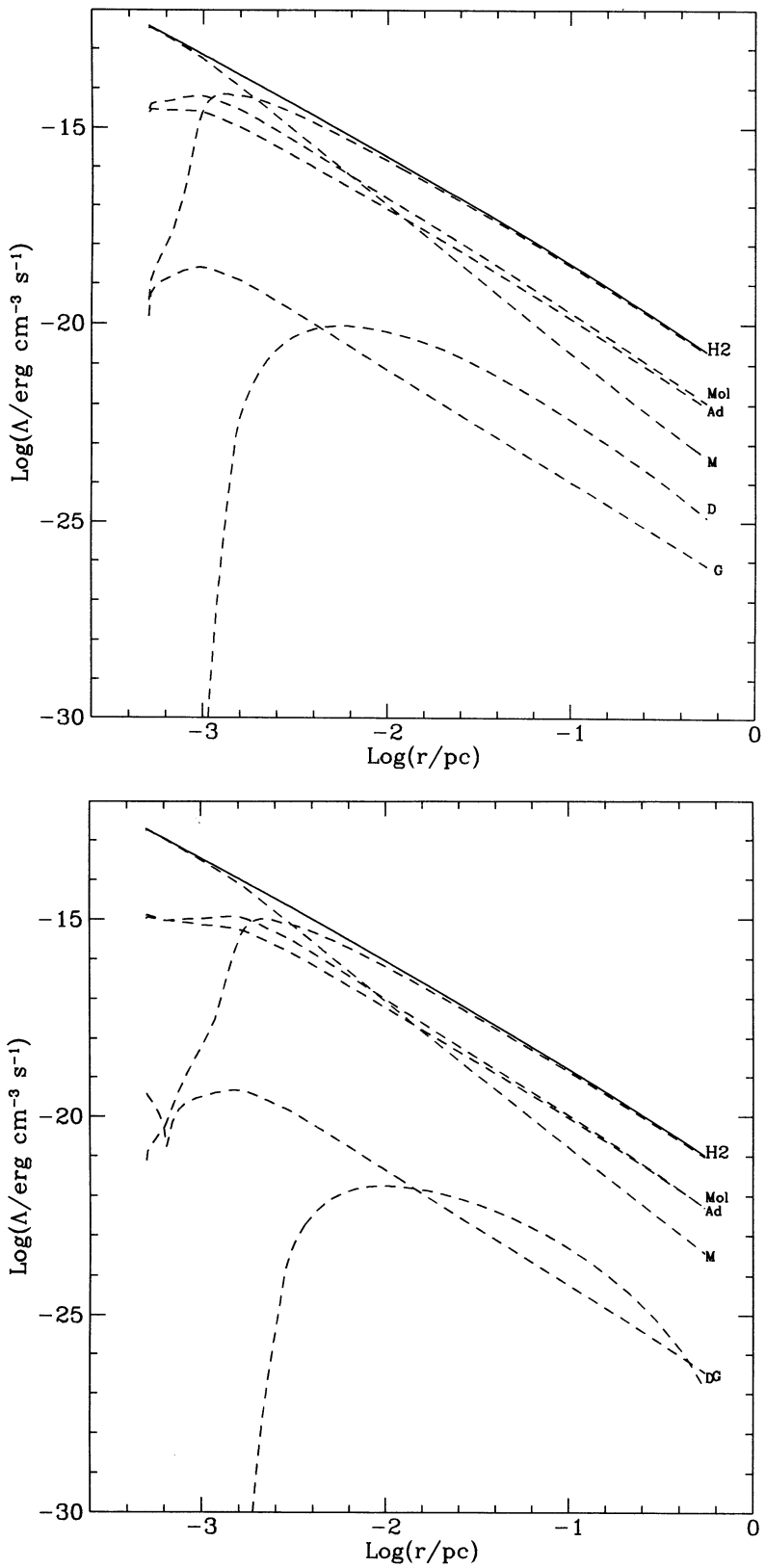

FIG. 3.—Heating and cooling functions for the different coolants as a function of r. Entrainment is the only heating source considered and is reported as the upper solid line. The various coolants are reported as dashed lines: (H2) rotational/vibrational emission of H_2; (Mol) rotational lines of molecules with dipole moments, including the first vibrational transition of OH and H_2O; (Ad) adiabatic expansion; (M) atomic cooling, includes H, He, and metals (allowed and forbidden transitions); (D) dissociation of H_2; (G) dust grains cooling. All radiative coolings are treated in an optically thin approximation. The upper panel shows the model with heating factor $\eta = 1.0$; the lower panel shows the case for $\eta = 0.5$.

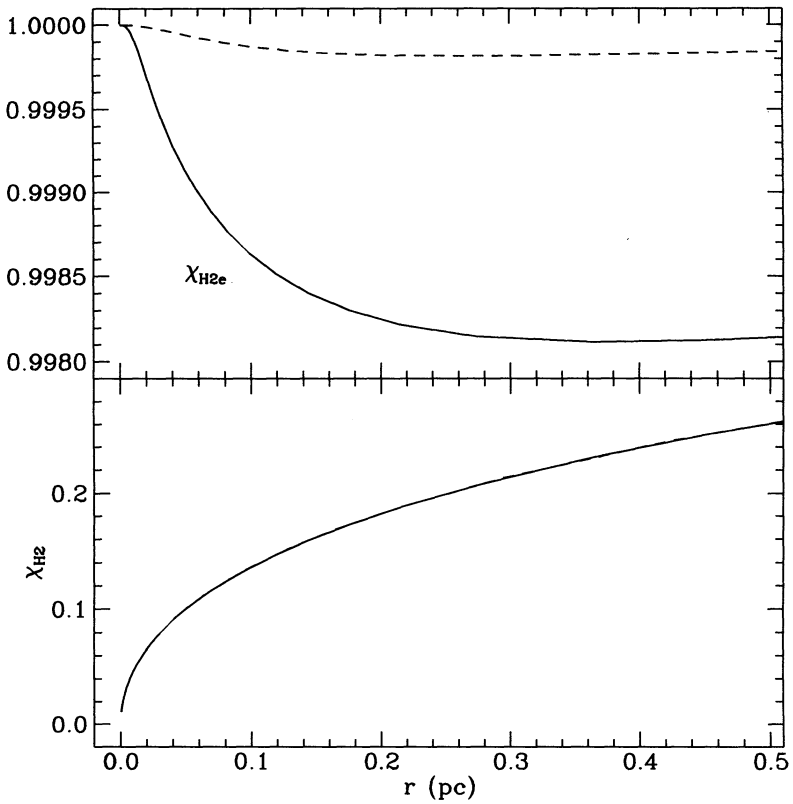

FIG. 4.—The upper panel shows the entrained molecular fraction χ_{H_2e}, that is, the ratio between molecular density ρ_{H2} and the contribution to the total density by the mass entrained up to that point $\chi_{H_2e} = \rho_{H2}/\rho_{entrained}$ as a function of r. The solid line is for a heating factor $\eta = 1.0$ and the broken line for $\eta = 0.5$. Almost no dissociation occurs. The lower panel shows the behavior of the molecular fraction $\chi_{H2} = \rho_{H2}/\rho$. Due to the low dissociation rate, χ_{H2} increases steadily with r because of the entrainment of molecular material in the mixing layer.

imation (see Appendix) with $\tilde{\alpha} = 1$ and $\tilde{\beta} = 0.05$, which is the sticking coefficient on graphite grains estimated at temperatures of the order of thousands of degrees (Leitch-Devlin & Williams 1985). The broken curve is for a heating factor $\eta = 0.5$, and the solid one for $\eta = 1.0$ in equation (6). For a maximum sticking coefficient $\tilde{\beta} \sim 1$, the dust can warm up a bit to ~ 15 K, but, due to the effective H_2 line cooling, the gas temperature is not sensitive to the behavior of T_{gr} and, therefore, largely independent of any particular choice of the dust accommodation factors introduced in the Appendix.

5. DISCUSSION

Given the results of the previous section, we can estimate the energy flux that should be observed as extended H_2 line emission in the mixing layer of L1551. The emission is extended (see discussion below) because, as shown by Figure 1, it would come from the region between two cones with opening angles 12° and 20°, respectively, that extends radially up to 0.5 pc (Paper I).

In the approximation of excitation by collisions with molecular and atomic hydrogen, Figure 6 illustrates the behavior of the H_2 line cooling functions for a heating factor $\eta = 0.5$ in equation (6). The upper panel shows the integrated luminosity of the total H_2 rovibrational cooling (*solid line*); the $v = 1 \rightarrow 0$ $S(1)$ line cooling (*dotted line*); and the $v = 2 \rightarrow 1$ $S(1)$ line cooling (*broken line*). The integration extends over the intercone region occupied by the mixing layer. The lower panel shows the local contribution of these two lines to the total H_2 line cooling function. For $\eta = 1$, the $v = 1 \rightarrow 0$ $S(1)$ line emission is 2.3 higher than that of the $\eta = 0.5$ model because all the entrainment energy goes into thermal energy and the gas temperature is higher (see Fig. 5). The $v = 2 \rightarrow 1$ $S(1)$ line emission is 5.9 higher than that of the $\eta = 0.5$ model. The total integrated luminosity (up to 0.5 pc) is then $L_{1\rightarrow 0} = 0.16$–$0.35\ L_\odot$, depending on the value of η. At a distance of 140 pc for L1551, this implies a flux, $F_{v=1\rightarrow 0} \sim 5 \times 10^{-10}$ ergs s^{-1} cm^{-2}. This flux is emitted over almost all of the intercone region which has an extension of ~ 36 arcmin^2 in the sky. This diffuse emission is within the detection limits of current, low spatial resolution, NIR spectrographs (D. Jaffe, private communication).

Note that, since the stellar wind does not decelerate to $v = 0$ at the end of the cones, the kinetic energy of the wind has to be dissipated at the end of the CO lobes, probably in a shock (see discussion in Paper I). In particular, for L1551, $L_w = \frac{1}{2}\dot{M}_w v_w^2 \sim 5.5\ L_\odot$. Shock models, applied to the physical conditions in this region, are needed to find the line emission in the shock. It is interesting to note that H_2 emission has been observed in this type of "terminal shocks" in IRAS 03282+3035 (Ballu et al. 1993) and a number of other sources.

It has been proposed that high-velocity molecular outflows may be due to entrained material in the wake of the bow shock of a collimated jet (Raga & Cabrit 1993; Masson & Chernin 1993; Chernin et al. 1994; Raga et al. 1994). Observations of bright molecular hydrogen 2.122 μm emission associated to HH objects (see, e.g., the reviews of Lane 1989; Curiel 1992; Eislöffel et al. 1994), and young molecular outflows (e.g., Bally, Lada, & Lane 1993b; Bally et al. 1993a) seem to agree qualitatively with this model. In contrast, the model studied in this

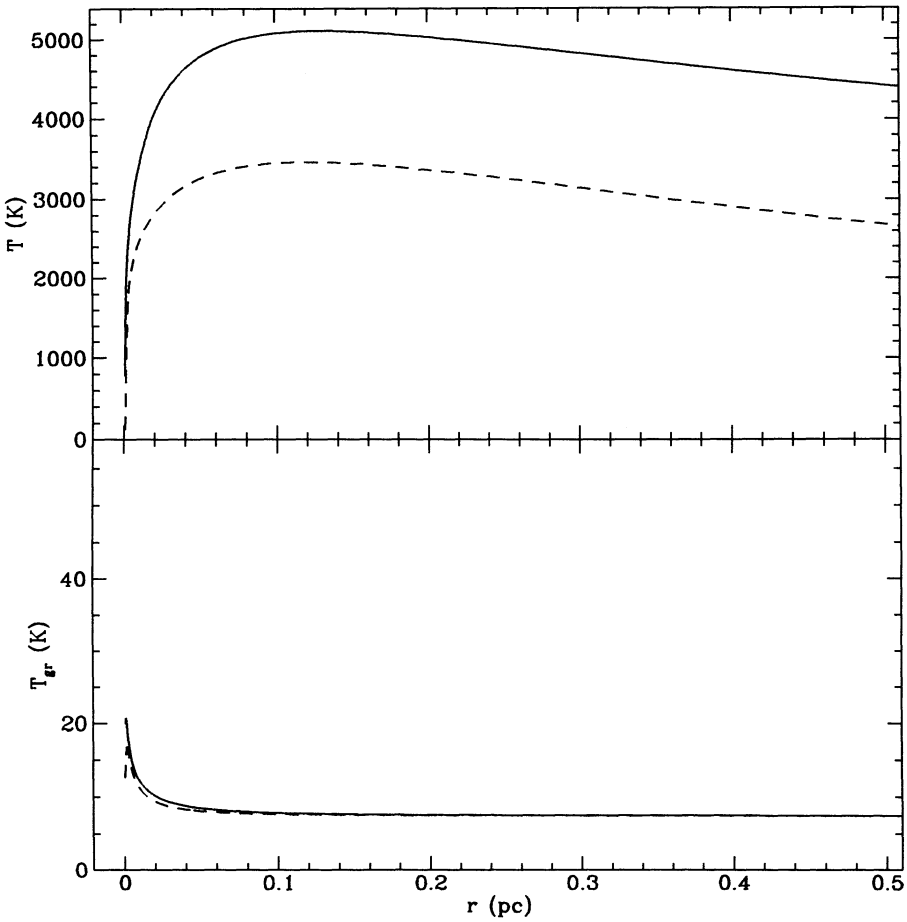

FIG. 5.—The upper panel shows the gas temperature T as a function of distance to the origin, and the lower panel shows the dust temperature T_{gr}. Due to the low density, grains remain cold because the transfer of energy by collision with gas particles is not effective. This particular model assumes that only sticking events contribute to the gas-dust thermal coupling; the sticking coefficient is $\tilde{\beta} = 0.05$. The solid line is for a heating factor $\eta = 1.0$, while the broken line corresponds to $\eta = 0.5$.

work corresponds to a well-developed, extended mixing layer of the type first studied by CR91, that would correspond to what is observed as the CO lobe in the classical source L1551. This source, which is a prototype of the CO outflow sources, has extended CO lobes and an observed atomic wind such that the H I line profiles can be reproduced by a freely flowing conical stellar wind plus an extended zone of deceleration as described in Paper I. As discussed above, this type of mixing layer should produce a very low surface brightness H_2 emission.

Finally, in a recent work, Taylor & Raga (1994) modeled the chemistry of a plane mixing layer of the type studied by CR91. They found that the layer has a very high temperature $\sim 10^4$ K and emits mostly in vibrational and rotational lines of H_2. At the end, as the mixing layer increases in width, the energy of the entrainment process is deposited in a larger area and the temperature drops to thousands of degrees. This result is in agreement with our model which considers a rather wide mixing layer. Their model applies to objects with thinner mixing layers, hence closer to the central source, while ours is appropriate to describe sources with more extended mixing layers, at larger distances from the source.

6. CONCLUSIONS

We explore the possibility that stellar winds interact with the ambient cloud through entrainment of molecular material. We determine the energy balance and the thermal structure of the entrainment region. This entrainment region, that is, the region of interaction between the wind and the ambient cloud, is modeled as a mixing layer along the walls of a cavity within the cloud itself. We make use of the 21 cm H I spectral profiles observed in L1551 to specify a priori the overall geometry of the flow and the amount of entrainment at each point. Assuming momentum conservation in the layer, we then determine—in a single parcel approximation—the radial temperature profile of the mixing layer.

We find that, with a reasonable choice of assumptions, the temperature in these regions is between 3000 and 5000 K. This results from heating due to the dissipation of wind kinetic energy as it decelerates outward due to mass entrainment, and from cooling by rovibrational emission of molecular hydrogen. In fact, because of the low density, short crossing time, and replenishment from the cloud, the H_2 is not dissociated and acts as the main coolant in the layer. Even taking into account the possibility of high relative velocity between gas and dust grains, we find that, due to the low density in most of the layer, the thermal coupling between the two phases is low. Consequently, the dust is much cooler than the gas ($T_{gr} < 20$ K), and it is not an efficient coolant of the medium.

In the case of L1551, the H_2 emission from the mixing layer comes from a large spatial area, more or less coextensive with the CO lobes. Nevertheless the flux in line emission of the H_2

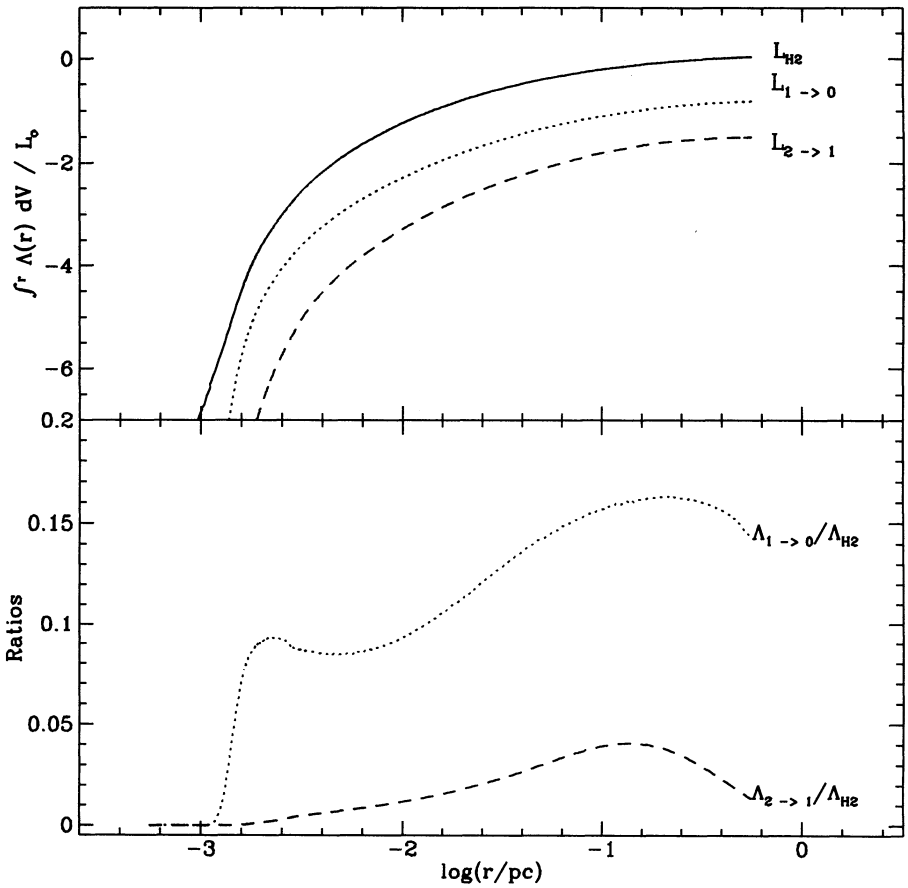

FIG. 6.—The upper panel shows the integrated luminosity for the case $\eta = 0.5$ of total H_2 line cooling (*solid line*); $v = 1 \rightarrow 0$ $S(1)$ line cooling (*dotted line*); and $v = 2 \rightarrow 1$ $S(1)$ line cooling (*broken line*). The integration extends over the intercone region occupied by the mixing layer. The lower panel shows the local ratios of the cooling function of the $v = 1 \rightarrow 0$ $S(1)$ line over the total H_2 line cooling function (*dotted line*), and the cooling function of the $v = 2 \rightarrow 1$ $S(1)$ line over the total H_2 line cooling function (*broken line*).

transition $v = 1 \rightarrow 0$ $S(1)$ should be within the limit of detection of current (arcminute resolution) near-infrared spectrographs, if extinction permits.

The physics of the mixing layers is not well established theoretically. For the conditions in stellar winds in molecular clouds, the following questions remain: How is the mass transported in this region? Could intermittency or thermal instabilities explain the clumpiness observed (see, e.g., review by Bachiller & Gómez-Gónzalez 1992) in the high-velocity molecular gas? and Does it have a smooth deceleration or is it a chaotic one with shocks? The modeling presented here is mainly aimed to a simple and approximate estimate of the heating due to the entrainment process and of the resulting radial thermal structure. In particular, the identification of the main cooling processes is these regimes is relevant to more detailed studies, such as full hydrodynamical simulations, which need a compact treatment of the energetics involved.

We thank A. Arrieta, J. Cantó, D. Chernoff, V. Escalante, J. Franco, A. Natta, F. Palla, F. Rubini, M. Walmsley, A. Dalgarno, and A. Raga for helpful discussions. This research was financed by CONACYT 0122-E and UNAM/DGAPA 100291.

APPENDIX

DUST COOLING

In our calculations we assume spherical dust grains of uniform radius $a = 0.05$ μm, mass density $\rho_g = 3$ cm^{-3}, and a mass ratio between dust and gas of 0.6×10^{-2}.

In the case of neutral grains, and neglecting radiation pressure, a grain injected at rest in a wind flowing with $v = 200$ km s^{-1} and with a mass-loss rate $\dot{A}_1 = 10^{-6}\ M_\odot$ yr^{-1} sr^{-1} will have an acceleration time of the order of 4000 yr, comparable to the radial crossing time of the flow region, and it will move a distance of 0.3 pc. This implies that neutral grains will not be at rest with respect to the flow and the impact velocity of the flow particles on them will deviate from the thermal one. For simplicity, given the similarity between acceleration and crossing times, we assume a relative streaming velocity between gas and dust equal to half the local flow velocity. In such conditions even the impact energies of H atoms will easily exceed 100 eV and will have a considerable sputtering efficiency. By using the nonthermal sputtering rates compiled by Tielens et al. (1994), we calculate a grain destruction

time in excess of 10^4 yr, that is, considerably longer than the radial crossing time and, therefore, we neglect any destruction mechanism for the grains.

We assume that the stellar wind is dust free and that the dust in the mixing layer is contributed only by entrained material. The dust content is then described by a continuity equation similar to equation (7), without the destruction term $D(r)$.

The radiation losses (ergs s^{-1}) of a dust grain at temperature T_{gr} and with a λ^{-1} absorption coefficient can be written as

$$R(T_{gr}) = \pi a^2 \epsilon_d 4\pi \int_0^\infty B_\nu(T_{gr}) \frac{2\pi a}{\lambda} d\nu , \tag{A1}$$

where ϵ_d is an efficiency factor. For $\lambda \sim 150$ μm, adequate for emission at $T_{gr} \simeq 20$ K, and assuming Mie scattering with an average refractive index $m(150\ \mu\text{m}) = 3.0 - i0.50$, we obtain in the Rayleigh limit $\epsilon_d = 0.29$. Given the uncertainties on grain size, shape, and composition, our calculations were performed assuming $\epsilon_d = 1$.

The collisional energy exchange rate between the grain and the ambient gas (H I + H_2) is given by

$$G(T_{gr}) = \pi a^2 2k(T_{eff} - T_{gr})(n_H v_{imp}^H + n_{H_2} v_{imp}^{H_2}) , \tag{A2}$$

where T_{eff} is an effective temperature of the gas, n_H and n_{H_2} are the number densities of atoms and molecules, and v_{imp} is the average impact velocity of the flow particles on the grain. In case of purely thermal motions, that is, if the grain is at rest with respect to the gas bulk motion, T_{eff} equals the gas temperature T and $v_{imp} = (8kT/\pi\mu)^{1/2}$, μ being the molecular weight of the gas particle.

If v_s is the gas streaming velocity relative to the grain, we define the ratio $s = (\mu v_s^2/2kT)^{1/2}$ and the average impact velocity will be $v_{imp} \sim (8kT/\pi\mu)^{1/2}(1 + \pi s^2/4)^{1/2}$, which is exact in the limits of purely thermal and purely streaming motion. Assuming that the impinging particles do not stick to the grain, Draine (1980) approximates the energy exchange as $2k(T_{eff} - T_{gr}) \sim 2k\tilde{\alpha}[T(1 + s^2/2) - T_{gr}]$, where $\tilde{\alpha}$ is an accommodation factor independent of the impact energy. Since it is more likely that only a fraction of the impacts, namely those with lower energy, will actually result in nonelastic scatterings, we introduce two accommodation factors: one, $\tilde{\alpha}$, for the contribution of nonthermal motion, and the other, $\tilde{\beta}$, for the probability of nonelastic scattering. In this case $v_{imp} \sim \tilde{\beta}(8kT/\pi\mu)^{1/2}(1 + \tilde{\alpha}\pi s^2/4)^{1/2}$ and $2k(T_{eff} - T_{gr}) \sim (3/2)k[T(1 + \tilde{\alpha}s^2/2) - T_{gr}]$, where only translational energy is taken into account. In this way it is possible to accommodate a number of gas-dust interactions, e.g., if only sticking events are assumed to contribute to the thermal coupling, $\tilde{\alpha} = 1$ and $\tilde{\beta}$ equals the sticking coefficient.

Neglecting the dust heat capacity, the grain temperature T_{gr} results from the balance

$$G(T_{gr}) = R(T_{gr}) - \Gamma_B , \tag{A3}$$

where we include in Γ_B the heating due to background radiation and to diluted radiation from the central star. The background field is specified by a temperature T_B, the star radiation by a photospheric temperature T_*, and a dilution coefficient $d_* = 0.5(r/r_*)^2$, where $r_* = 3\ R_\odot$ (we neglect any extinction of the stellar radiation). The term $G(T_{gr})$, upon sign reversal, also determines the dust contribution to the gas cooling function Λ in equation (5).

We neglect in our treatment of the gas-dust interaction the influence of drag forces on the gas dynamics which, in our scheme, is largely dominated by the inertial braking due to mass entrainment in the flow.

REFERENCES

Bachiller, R., & Cernicharo, J. 1990, A&A, 239, 276
Bachiller, R., & Gómez-Gónzalez, J. 1992, Astron. Astrophys. Rev., 3, 257
Bally, J., Devine, D., Hereld, M., & Rauscher, B. J. 1993a, ApJ, 418, L75
Bally, J., Lada, E. A., & Lane, A. P. 1993b, ApJ, 418, 322
Bally, J., & Lane, A. P. 1991, in The Physics of Star Formation and Early Stellar Evolution, ed. C. J. Lada & N. D. Kylafis (Dordrecht: Kluwer), 471
Bally, J., & Stark, A. A. 1983, ApJ, 266, L61
Cantó, J., & Raga, A. 1991, ApJ, 372, 646 (CR91)
Chernin, L., Masson, C., Gouveia dal Pino, E. M., & Benz, W. 1994, ApJ, 426, 204
Curiel, S. 1992, in IAU Symp. 150, Astrochemistry of Cosmic Phenomena, ed. P. D. Singh (Dordrecht: Kluwer), 373
Dalgarno, A., & McCray, R. A. 1972, ARA&A, 10, 375
Dove, J. E., & Mandy, M. E. 1986, ApJ, 311, L93
Eislöffel, S., Davis, C. J., Ray, T. P., & Mundt, R. 1994, ApJ, 422, L91
Giovanardi, C., Lizano, S., Natta, A., Evans, N. J., II, & Heiles, C. 1992, ApJ, 397, 214 (Paper I)
Herbig, G. H. 1962, Adv. Astr. Ap., 1, 47
Hollenbach, D., & McKee, C. F. 1979, ApJS, 41, 555
———. 1989, ApJ, 342, 306
Koo, B.-C. 1989, ApJ, 337, 318
Lada, C. J. 1985, ARA&A, 23, 267
Lane, A. P. 1989, in ESO-Workshop on Low Mass Star Formation and Pre–Main-Sequence Objects, ed. B. Reipurth (Garching: ESO), 331
Leitch-Devlin, M. A., & Williams, D. A. 1985, MNRAS, 213, 295
Lepp, S., & Shull, J. M. 1983, ApJ, 270, 578
Lizano, S., Heiles, C., Rodríguez, L. F., Koo, B.-C., Shu, F., Hasegawa, T., Hayashi, S., & Mirabel, I. F. 1988, ApJ, 328, 763
Masson, C., & Chernin, L. 1993, ApJ, 414, 230
Mac Low, M.-M., & Shull, J. M. 1986, ApJ, 302, 585
McKee, C. F., Storey, J. W. V., Watson, D. M., & Green, S. 1982, ApJ, 259, 647
Natta, A., Giovanardi, C., Palla, F., & Evans, N. J., II 1988, Ap, 327, 817
Neufeld, D., & Kaufman, M. J. 1993, ApJ, 418, 263
Rawlings, J. M. C., Williams, D. A., & Cantó, J. 1988, MNRAS, 230, 695
Raga, A., & Cabrit, S. 1993, A&A, 278, 267
Raga, A., Taylor, S., Cabrit, S., & Biro, S. 1994, preprint
Rodríguez, L. F., Lizano, S., Cantó, J., Escalante, V., & Mirabel, I. F. 1990, ApJ, 365, 261
Ruden, S. P., Glassgold, A. E., & Shu, F. H. 1990, ApJ, 361, 546
Ruiz, A., Alonso, J. L., & Mirabel, F. 1992, ApJ, 394, L57
Russell, A. P. G., Hills, R. E., Padman, R., & Bally, J. 1992, ApJ, 287, 219
Shu, F. H., Adams, F. C., & Lizano, S. 1987, ARA&A, 25, 23
Snell, R. L., Loren, R. B., & Plambeck, R. L. 1980, ApJ, 239, L17
Spitzer, L. 1978, Physical Processes in the Interstellar Medium (New York: John Wiley & Sons)
Taylor, S., & Raga, A. 1994, preprint
Tielens, A. G. G. M., McKee, C. F., Seab, C. G., & Hollenbach, D. J. 1994, ApJ, 431, 321